Mechanical and thermodynamical stability of $BiVO_4$ polymorphs using first-principles study

A K M Farid Ul Islam[1,†], Md Nurul Huda Liton[2], H M Tariqul Islam[3], Md Al Helal[2], and Md Kamruzzaman[4]

[1] *Department of Computer Science and Engineering, Begum Rokeya University, Rangpur, Rangpur-5400, Bangladesh*
[2] *Department of Physics, Begum Rokeya University, Rangpur, Rangpur-5400, Bangladesh*
[3] *Department of Chemistry, Begum Rokeya University, Rangpur, Rangpur-5400, Bangladesh*
[4] *Department of Physics and Materials Science and Center of Super-Diamond and Advanced Films (COSDAF), City University of Hong Kong, Hong Kong SAR, China*

(Received 9 June 2016; revised manuscript received 7 December 2016; published online 18 January 2017)

First principles calculations of structural, electronic, mechanical, and thermodynamic properties of different polymorphs of $BiVO_4$ are performed using Bender-type plane/wave ultrasoft pseudopotentials within the generalized gradient approximation (GGA) in the frame of density functional theory (DFT). The calculated structural and electronic properties are consistent with the previous theoretical and experimental results. The electronic structures reveal that m-$BiVO_4$, op-$BiVO_4$, and st-$BiVO_4$ have indirect band gaps, on the other hand, zt-$BiVO_4$ has a direct band gap. From the DOS and Mulliken's charge analysis, it is observed that only m-$BiVO_4$ has $6s^2$ Bi lone pair. Bond population analysis indicates that st-$BiVO_4$ shows a more ionic nature and a similar result is obtained from the elastic properties. From the elastic properties, it is observed that st-$BiVO_4$ is more mechanically stable than the others. st-$BiVO_4$ is more ductile and useful for high electro-optical and electro-mechanical coupling devices. Our calculated thermodynamic properties confirm the similar characteristics found from electronic and elastic properties. m-$BiVO_4$ is useful as photocatalysts, solid state electrolyte, and electrode and other polymorphs are applicable in electronic device fabrications.

Keywords: $BiVO_4$, crystal structure, lone pair, mechanical stability

PACS: 63.20.dk, 71.20.nr, 74.25.Ld, 73.22.–f **DOI:** 10.1088/1674-1056/26/3/036301

1. Introduction

At the present, finding an alternative energy source is a great demand due to the decreasing of available fossil and inadequate natural energy sources in the technology dependent world, which can also reduce environmental pollution. These limitations can be overcome by degrading toxic pollutants and splitting water for hydrogen production. To fulfill this purpose, photocatalyst may play an important role.

Since solar energy is one of the abundant energy sources, it can be widely used for electrical and thermal power generation. Due to the enormous sources of chemical energy such as H_2, as compared to electricity and its environmental stability and potentially higher efficiency solar cell is able to make a concentration as one of the promising technological concepts. It is well known that wide band gap semiconductors, such as TiO_2 (3.2 eV) and ZnO (3.4 eV), are extensively used as photocatalysts.[1,2] The control of both sizes and shapes of semiconductor photocatalysts is very important for their photocatalytic activity because the photocatalytic reaction occurs at the interface between photocatalyst and electrolyte. However, the utilization of solar energy, i.e., the solar cell efficiency, is greatly affected by the mismatch between the large band gap of the semiconductor and the sunlight spectrum. TiO_2 and ZnO based solar cells are effective only in the ultraviolet region (utilization of about 4% of the sunlight energy). Therefore, a photocatalyst with a narrow band gap responding to visible light is highly desired.

Ti-free narrow band gap semiconducting oxides containing bismuth, such as $BiVO_4$, Bi_2WO_6, and $BiMoO_6$, have recently received a great deal of attention because of their visible light responsive photocatalytic activities.[3–8] Among these materials, $BiVO_4$ is one of the most active O_2 evolution photocatalyst in the field of semiconductor and photoelectrode[3,6] due to its relatively low band gap of about 2.4 eV, enabling it to the more efficient use of visible light and an adequate position of the conduction and valance bands as compared to the oxidation potential of water.[6] In addition, $BiVO_4$ is a relatively abundant,[6,8] non-toxic material[9] and it also displays various interesting and desirable physical properties, such as ionic conductivity[10] and ferro-elasticity.[11]

There are different polymorphs of $BiVO_4$, the well known polymorphs are monoclinic clinobisvanite (m-$BiVO_4$), orthorhombic pucherite (op-$BiVO_4$), zircon tetragonal dreyerite (zt-$BiVO_4$), and scheelite tetragonal (st-$BiVO_4$).[5,12] Among them, m-$BiVO_4$ with a band gap of 2.4 eV shows higher photocatalytic activity for O_2 evolution, chemical reaction induced visible light irradiation, photo decomposition of organic pollutants, water decomposition, carbon dioxide re-

†Corresponding author. E-mail: farid_ru@yahoo.com

© 2017 Chinese Physical Society and IOP Publishing Ltd

duction, and generation of photo-current.[3–5,13–19] Several methods, such as solid-state reaction, co-precipitation, hydrothermal treatment, chemical bath deposition, organometallic decomposition, and sonoechemical routes have been reported for the fabrication of $BiVO_4$.[11,16,20–23] Aqueous, hydrothermal, and solvothermal processes are different solution based methods that have been developed to fabricate m-$BiVO_4$ nanostructures, such as nanoellipsoids,[24–26] nanowires/nanofibers,[27,28] nanosheets/nanoplates,[29,30] hyperbranched crystals,[31] and mesocrystals.[32]

On the other hand, recent high quality experimental results highlighted that the photo-electrochemical (PEC)-induced oxidation under visible light irradiations represents a challenging test of modern electronic structure of $BiVO_4$.[18,33–36] The electronic and optical properties of $BiVO_4$ are studied by using density function theory (DFT) and these studies show that it is a direct band gap material with a band gap of 2.16 eV.[15,37] UV–vis spectra suggest that $BiVO_4$ has a dipole-allowed direct band gap,[18,38] but the experimental value is 2.4 eV.[3,5,16,39–42] Several authors recently studied its electronic properties introducing GGA with PBSol,[43] hybrid functions (HSE 06)[44–46] to improve the calculated energy band gap.

However, there is still an incomplete understanding of the physical properties of $BiVO_4$ that leads to a high photocatalytic activity as well as the formation process correlated with this phenomenon. To study the durability of photocatalyst, solid state electrolyte and electrode, we need to know the mechanical stability. Yuan *et al.*[47] reported on the pressure dependent mechanical stability, but there is no theoretical or experimental study on the thermodynamical stability of $BiVO_4$ polymorphs which will support many applications. Elastic properties of materials provide information regarding the bonding characteristics between crystal planes of the atoms and the anisotropic character of the bond is useful to determine the structural stability of the crystal. In addition, the thermodynamic properties of photocatalytic compounds are important because the Gibbs free energy, Debye temperature, and heat capacity can determine the thermodynamical stability of the system.

In this paper, we investigate the electronic structure, elastic and thermodynamic properties of $BiVO_4$ polymorphs and also study their interrelation using first principles calculations.

2. Computational details

The calculations were performed using the CASTEP code.[48] The geometrical structures and physical properties such as electronic, elastic, and thermodynamic properties were calculated with ultrasoft pseudopotential using density function theory (DFT).[49] We employed Perdew–Burke–Ernzerhof GGA[50] to calculate the exchange and correlation potentials. The valence configurations are $6s^2 6p^3$ for Bi, $2s^2 2p^4$ for O, and $3d^3 4s^2$ for V. Here, we considered two formula units of $BiVO_4$ in a primitive cell. The kinetic energy cutoff for the plane waves was 480 eV and the energy convergence criterion was chosen to be 10^{-6} eV. The maximum force on each atom and stress were less than 0.01 eV/Å and 0.05 GPa, respectively, and the displacement of atoms during the geometry optimization was less than 0.0005 Å. The Brillouin zone was sampled using the Monkhorst–Pack scheme with a $12 \times 12 \times 6$ k-point set.

3. Results and discussion

3.1. Crystal structure

The optimized lattice parameters of m-$BiVO_4$ (space group $I2/b$),[14] op-$BiVO_4$ (space group $Pnca$),[51] zircon tetragonal (zt-$BiVO_4$) (space group $I41/amd$),[52] and st-$BiVO_4$ (space group $I41/a$)[14] are tabulated in Table 1. Our optimized lattice parameters are consistent with the available theoretical[47,52,53] and experimental values.[14,51,54]

The basic unit structures of $BiVO_4$ polymorphs are shown in Figs. 1(a)–1(d). It is seen that V forms VO_4 tetrahedron for all polymorphs, whereas, Bi forms BiO_6 octahedron for m-$BiVO_4$, BiO_4 tetrahedron for zt-$BiVO_4$ and op-$BiVO_4$, and BiO_8 dodecahedron for st-$BiVO_4$. Some researcher reported that for m-$BiVO_4$, Bi forms BiO_8 dodecahedron,[54] but in our study Bi forms BiO_6 octahedron. This may happen due to the lone pair activity of Bi 6s electrons. This is the key factor for the electrical conductivity of m-$BiVO_4$. It is also seen that both m-$BiVO_4$ and op-$BiVO_4$ form a layered structure of Bi–V–O units stacked along the c-axis. On the contrary, there is no distinct Bi–O–V layer observed in zt-$BiVO_4$ and st-$BiVO_4$, because in these structures, Bi forms a bond with oxygen of the next Bi–O–V layer.

Table 1. Calculated, theoretical, and experimental lattice parameters of different $BiVO_4$ polymorphs.

Polymorphs	Present work				Theoretical[47,52,53]				Experimental[14,51,54]			
	a/Å	b/Å	c/Å	α,β,γ	a/Å	b/Å	c/Å	α,β,γ	a/Å	b/Å	c/Å	α,β,γ
m-$BiVO_4$	5.1684	5.1301	11.6887	$\alpha=\beta=90°$ $\gamma=89.8798°$	5.183	5.074	11.711	$\alpha=\beta=90°$ $\gamma=90.36°$	5.1935	5.0898	11.6972	$\alpha=\beta=90°$ $\gamma=90.398°$
op-$BiVO_4$	5.3863	5.0509	11.9070	$\alpha=\beta=\gamma=90°$	–	–	–	–	5.33	5.06	12.02	$\alpha=\beta=\gamma=90°$
zt-$BiVO_4$	7.3633	7.3633	6.4337	$\alpha=\beta=\gamma=90°$	7.350	7.350	6.434	$\alpha=\beta=\gamma=90°$	7.303	7.303	6.584	$\alpha=\beta=\gamma=90°$
st-$BiVO_4$	5.1496	5.1496	11.6380	$\alpha=\beta=\gamma=90°$	5.121	5.121	11.647	$\alpha=\beta=\gamma=90°$	5.147	5.147	11.7216	$\alpha=\beta=\gamma=90°$

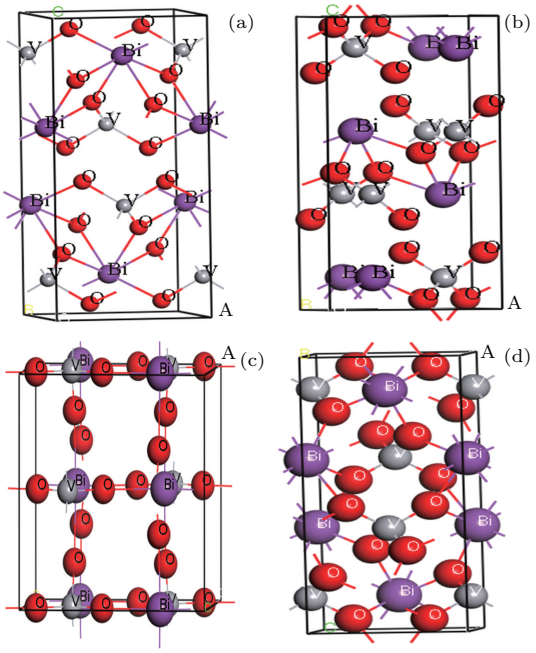


Fig. 1. (color online) Crystal structures of (a) m-$BiVO_4$, (b) op-$BiVO_4$, (c) zt-$BiVO_4$, and (d) st-$BiVO_4$.

3.2. Electronic structure

The investigation of the electronic band structure for understanding the electronic properties of $BiVO_4$ polymorphs is very useful. The band structure of $BiVO_4$ is shown in Figs. 2(a)–2(d). Here, the Fermi energy is set to zero. The energy band structures of $BiVO_4$ were calculated along the high symmetry points of the Brillioun zone. From our calculation, it is seen that the valence band maximum (VBM) is on the Z–G line for m-$BiVO_4$ and st-$BiVO_4$, the Y-line for op-$BiVO_4$, and the conduction band minimum (CBM) is located at the A-line for m-$BiVO_4$ and st-$BiVO_4$, and the X-line for op-$BiVO_4$. The observed indirect band gaps of m-$BiVO_4$, op-$BiVO_4$, and st-$BiVO_4$ are 2.193 eV, 2.461 eV, and 2.169 eV, respectively. Whereas, zt-$BiVO_4$ is a direct band gap material and its band gap is 2.598 eV. Its VBM and CBM are located on the G–Z line. Our calculated band gaps are consistent with the available theoretical values[15,37,47] but less than the experimental ones[3,5,16,39–42] due to the well-known underestimation of DFT.

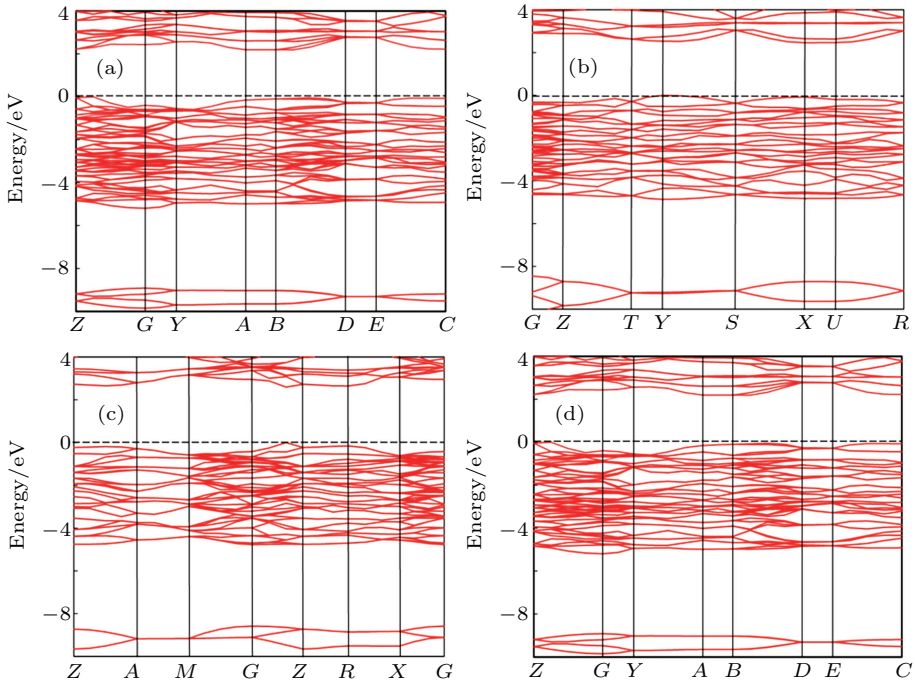


Fig. 2. (color online) GGA calculated band structures of (a) m-$BiVO_4$, (b) op-$BiVO_4$, (c) zt-$BiVO_4$, and (d) st-$BiVO_4$ along some high-symmetry lines in the Brillouin zone.

The total and partial densities of states corresponding to the electronic band structures of $BiVO_4$ polymorphs are shown in Figs. 3(a)–3(d). From the figure, it is observed that the upper valence band is spread between 0 and −5.5 eV with respect to the highest occupied states. In the upper valence band, the electronic character is mainly due to the O 2p state, which are the common characteristics of oxide semiconducting materials. The V 3d, Bi 6s and 6p states also contribute to the upper valence band. Although there are s, p, and d orbitals but only the p–d hybridization occurs at the top of the valence band. Since Bi 6s and O 2p show anti-bonding nature between −1.63 eV and −3.02 eV, we can say that Bi 6s acts as a lone pair, which may be confirmed from Mulliken charge analysis, bond populations, and also from the crystal structures. The energy bands at −7.0 eV to −10 eV and −16 eV to −18 eV are the deep level valence states which consist of Bi 6s and O 2s states. It is also observed that the conduction band is mainly derived from V 3d states with p–d hybridization among the V 3d, O 2p, and Bi 6p states.

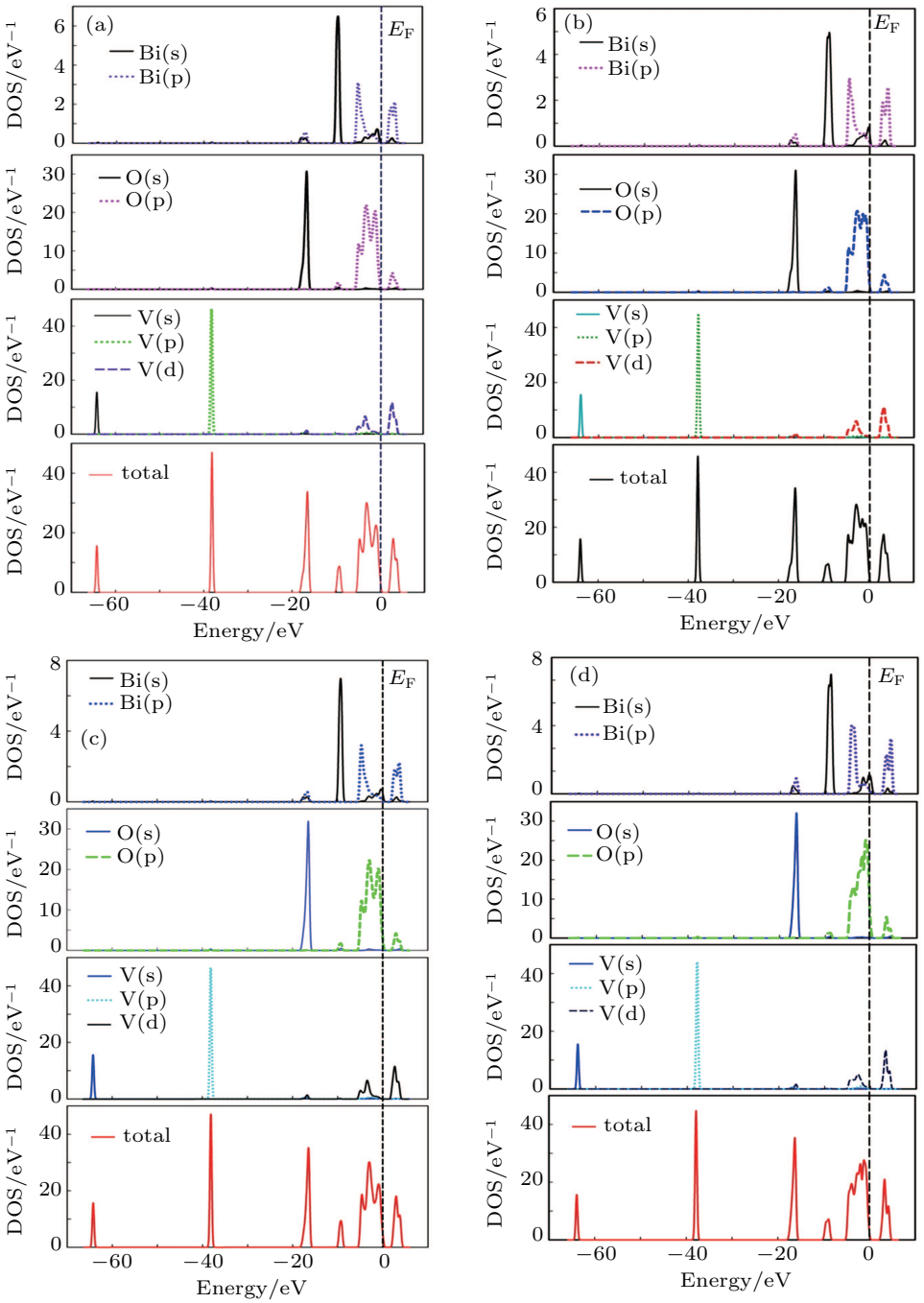


Fig. 3. (color online) Total DOS and PDOS of (a) m-$BiVO_4$, (b) op-$BiVO_4$, (c) zt-$BiVO_4$, and (d) st-$BiVO_4$ calculated by GGA.

The bonding behavior of $BiVO_4$ can be studied from the Mulliken charge analysis and bond populations. The atomic charges, chemical bond lengths, and bond populations are listed in Table 2. The higher value of charge transfer indicates higher overlap of the electron clouds of two bonding atoms, which causes ionic bonding. The higher value of bond population implies the strong covalency whereas the lower value exhibits the strong iconicity.

Table 2. Calculated bond length, bond population, charge, and band gap of different $BiVO_4$ polymorphs.

Polymorphs	Bond length	Population	Bond length	Population	Charge/e			Band gap/eV
	Bi–O/Å	Bi	V–O /Å	V	Bi	V	O	
m-$BiVO_4$	2.397, 2.402, 2.469, 2.575	0.06, 0.13, 0.05, 0.07	1.720, 1.761, 2.978	0.67, 0.61, –0.03	1.84	0.87	–0.71	2.193
op-$BiVO_4$	2.359, 2.380, 2.562, 2.616	0.16, 0.05, 0.03, –0.03	1.691, 1.791, 2.796	0.72, 0.54, 0.02	1.83	0.87	–0.75	2.461
zt-$BiVO_4$	2.399, 2.509	0.19, 0.05	1.728	0.66	1.87	0.89	–0.69	2.598
st-$BiVO_4$	2.439, 2.474	0.06, 0.10	1.739	0.64	1.85	0.87	–0.68	2.165

In all of the polymorphs of $BiVO_4$, the charge transfers from V and Bi to O are about 0.89 and 1.87 electrons, respectively, and the V–O bond populations (0.67, 0.72, 0.66, 0.64) are larger than those (0.13, 0.16, 0.19, 0.10) of the Bi–O bonds. Therefore, the strength of covalent bonding in the V–O bond is stronger than that in the Bi–O bond and the bonding behavior of $BiVO_4$ is mixed covalent-ionic, where m-$BiVO_4$ and op-$BiVO_4$ show relatively more covalency nature than the other polymorphs. From the crystal structure and electronic properties of $BiVO_4$, we conclude that the V atom makes both ionic and covalent bonds with O to form VO_4^{3+}, which confirms that no lone pair electron presents in the V atom but VO_4^{3+} creates an ionic bond with Bi^{3+} for $BiVO_4$. Therefore, we can say that V–O bonds are directly related to the interactive forces between Bi^{3+} and V^{5+}. However, in op-$BiVO_4$, zt-$BiVO_4$, and st-$BiVO_4$ structures, Bi shows +5 valency instead of +3 and there is no lone pair activity. From Table 2, it is also observed that the distortion of Bi–O bond length occurs due to $6s^2$ lone pair of Bi^{3+}. This characteristic plays an important role for the high photocatalytic activity of the visible light irradiation.[55] m-$BiVO_4$ may show more photocatalytic activities as compared to other $BiVO_4$ polymorphs.

3.3. Elastic properties

The calculated elastic coefficients and stiffness constants are tabulated in Table 3. The conditions of mechanical stability are important to estimate the stability of a compound. The calculated elastic constants of m-BiVO4 should satisfy the Born stability criterion[56,57] for monoclinic structure:

$C_{ii} > 0, (i = 1,2,3,4,5,6)$; $C_{11}+C_{22}+C_{33}+2(C_{12}+C_{13}+C_{33}) > 0$; $C_{33}C_{55}-C_{35}^2 > 0$; $C_{44}C_{66}-C_{46}^2 > 0$; $C_{22}+C_{33}-2C_{23} > 0$; $C_{22}(C_{33}C_{55}-C_{35}^2)+2C_{23}C_{25}C_{35}-C_{35}^2C_{55}-C_{35}^2C_{33} > 0$; $2(a_1C_{15}C_{25}+b_1C_{15}C_{35}+c_1C_{25}C_{35})-(d_1C_{35}^2+e_1C_{35}^2+f_1C_{35}^2)+g_1C_{55} > 0$;
where

$$a_1 = C_{33}C_{12}-C_{13}C_{23}, \quad b_1 = C_{22}C_{13}-C_{12}C_{23},$$
$$c_1 = C_{11}C_{23}-C_{12}C_{13}, \quad d_1 = C_{22}C_{33}-C_{13}^2,$$
$$e_1 = C_{11}C_{33}-C_{13}^2, \quad f_1 = C_{11}C_{22}-C_{12}^2,$$
$$g_1 = C_{11}C_{22}C_{33}-C_{11}C_{23}^2-C_{22}C_{13}^2-C_{33}C_{12}^2+2C_{12}C_{13}C_{23}.$$

Similarly, for the orthorhombic crystal, the mechanical stability conditions are[58,59]

$C_{11}+C_{22}-2C_{12} > 0$; $C_{11}+C_{33}-2C_{13} > 0$; $C_{22}+C_{33}-2C_{23} > 0$; $C_{ii} > 0$ $(i = 1,2,3,4,5,6)$; $C_{11}+C_{22}+C_{33}+2(C_{12}+C_{13}+C_{33}) > 0$.

For the tetragonal crystal, the mechanical stability conditions are[60]

$C_{11}-C_{12} > 0$; $C_{11}+C_{33}-2C_{13} > 0$; $C_{ii} > 0$ $(i = 1,3,4,6)$; $2C_{11}+C_{33}+2C_{12}+4C_{13}) > 0$.

By using the calculated data, it is seen that the elastic constants satisfy the above criteria, so we can say that m-$BiVO_4$, op-$BiVO_4$, zt-$BiVO_4$, and st-$BiVO_4$ are mechanically stable.

Table 3. Calculated elastic constants C_{ij} of different $BiVO_4$ polymorphs.

Polymorphs	C_{11}	C_{22}	C_{33}	C_{44}	C_{55}	C_{66}	C_{12}	C_{13}	C_{15}	C_{23}	C_{25}	C_{35}	C_{46}
m-$BiVO_4$	173.72	201.97	154.27	52.58	48.31	65.70	93.94	68.89	0.72	73.21	–0.81	–0.56	9.98
op-$BiVO_4$	133.87	237.90	201.46	39.63	29.86	62.65	68.49	49.10	–	78.39	–	–	–
zt-$BiVO_4$	182.58	–	253.62	39.99	–	17.16	37.22	79.78	–	–	–	–	–
st-$BiVO_4$	206.96	–	193.95	53.72	–	79.50	106.45	92.65	–	–	–	–	–

Voigt,[61] Reuss and Angew[62] separately proposed the average relations expressing the strain in terms of the given stress. Hill[63,64] proved that the approximations made by Voigt and Reuss represent the upper and lower bounds of the elastic constants, respectively. The resulting Voigt and Reuss moduli are expressed in terms of the stiffness constants C_{ij} and compliances S_{ij}, respectively. In particular, the bulk and shear moduli in the Voigt approach are

$$B_{\rm v} = \frac{1}{9}[C_{11}+C_{22}+C_{33}+2(C_{12}+C_{13}+C_{33})],$$
$$G_{\rm v} = \frac{1}{15}[(C_{11}+C_{22}+C_{33})-(C_{12}+C_{13}+C_{33}) +3(C_{44}+C_{55}+C_{66})].$$

The corresponding expressions for the Reuss procedure are

$$B_{\rm R} = [S_{11}+S_{22}+S_{33}+2(S_{12}+S_{13}+S_{23})]^{-1},$$
$$G_{\rm v} = 15[(4S_{11}+S_{22}+S_{33})-4(S_{12}+S_{13}+S_{23}) +3(S_{44}+S_{55}+S_{66})]^{-1}.$$

Thus, the Hill-averaged bulk ($B_{\rm H}$) and shear ($G_{\rm H}$) moduli can be determined by using

$$G_{\rm H} = \frac{1}{2}(G_{\rm v}+G_{\rm R}), \quad B_{\rm H} = \frac{1}{2}(B_{\rm v}+B_{\rm R}).$$

By using these average values of B and G, the Young modulus E and the Poisson ratio ν can be computed by the following equations:

$$E = \frac{9BG}{3B+G}, \quad \nu = \frac{3B-2G}{2(3B+G)}.$$

All the calculated elastic constants are shown in Table 4 for different crystal systems of $BiVO_4$. The bulk modulus B is a measure of resistance to volume change by applied pressure and it is related to the bond length.[65] From our calculation, it is seen that the order of bulk moduli is st > m > zt > op-$BiVO_4$, hence st-$BiVO_4$ has stronger resistance to the volume change caused by applied pressure than the other polymorphs of $BiVO_4$. From this point of view, st-$BiVO_4$ is more useful for hard coating than the others. On the other hand, high bulk modulus indicates the strong strength of the bonds in the solid.

Table 4. Calculated bulk modulus B (GPa), shear modululs G (GPa), Young's modulus E (GPa), G/B, Poisson ratio υ, anisotropy factors A_1, A_2, and A_3, Klemman parameter ξ, and Vicker's hardness H_v of different $BiVO_4$ polymorphs. The subscripts V, R, H, and V represent the Voigt, Reuss, Hill, and Vicker approximations, respectively.

Polymorphs	B_v	G_v	B_R	G_R	G_H	B_H	E	G/B	υ	A_1	A_2	A_3	ξ	H_v
m-$BiVO_4$	111.34	52.91	108.52	51.28	52.10	109.93	134.97	0.474	0.295	1.116	0.921	1.399	0.66	5.43
op-$BiVO_4$	107.24	51.58	98.52	46.06	48.82	102.88	126.46	0.475	0.295	0.669	0.423	1.067	0.63	5.13
zt-$BiVO_4$	112.48	47.56	105.45	36.30	41.93	108.97	111.49	0.385	0.330	0.578	–	1.647	0.36	2.82
st-$BiVO_4$	132.38	58.46	131.89	54.20	56.33	132.13	147.96	0.426	0.313	0.997	–	1.917	0.64	4.80

Shear modulus G is a quantity for measuring the stiffness of a material, which is also a measure of resistance to reversible deformation upon shear stress. Larger shear modulus indicates that the directional bonding between atoms is more pronounced.

Materials with high B and G are likely to be hard materials. The ratio of G/B gives the information about covalent and ionic behavior of materials on the basis of their brittle and ductile character in solids.[66] The upper limits of G/B are 1.1 for brittle and 0.6 for ductile character, i.e., if $G/B \leq 0.6$, the materials are ductile (ionic), otherwise brittle (covalent) in nature.

The ductility/brittleness is very important in the battery fabrication, since the electrode/electrolyte interface contact is crucial for better electrical conductance. Ductile electrode/electrolyte material can be able to change its shape without fracture. Ductile electrolyte material demonstrates good performance in terms of device fabrication, cycling performance, and safety.

From our calculation, it is observed that $BiVO_4$ polymorphs are ductile in order of st > m > zt > op-$BiVO_4$. Therefore, st-$BiVO_4$ shows more ductility and no fracture will occur readily upon mechanical pressure when it is used as solid state electrolyte.

The Young modulus E is important for technological and engineering applications. The larger E indicates more stiffer materials. High E indicates higher binding energies and shorter interatomic bond length in the materials.[67] Hence st-$BiVO_4$ is stiffer than the other three.

The Poisson ratio measures the degree of directionality of the covalent bonds. The Poisson ratio is small ($\nu = 0.1$) for a covalent material; where as it is greater than or equal to 0.25 for ionic materials. The Poisson ratio also reflects the stability of the crystal against shear. The values 0.25 and 0.5 are the lower and upper limits, respectively for central force in solids. In the present calculation, the Poisson ratios are 0.295, 0.295, 0.330, and 0.313 for m-$BiVO_4$, op-$BiVO_4$, zt-$BiVO_4$, and st-$BiVO_4$, respectively at zero pressure. This result reveals that the ionic contribution is dominated in these compounds, which makes them useful for high electro-optical and electromechanical coupling.[68] The obtained Poisson ratio indicates that all $BiVO_4$ have central interatomic forces.

The anisotropy of a material is another important parameter used to determine whether the structural properties are the same in all directions or not. In practice, all single crystals are anisotropic, so an appropriate parameter is needed to characterize the extent of anisotropy. For orthorhombic and monoclinic structures, the shear anisotropic factors are[69]

$$A_1 = A_{\{100\}} = \frac{4C_{44}}{C_{11}+C_{33}-2C_{13}},$$
$$A_2 = A_{\{010\}} = \frac{4C_{55}}{C_{22}+C_{33}-2C_{23}},$$
$$A_3 = A_{\{001\}} = \frac{4C_{66}}{C_{11}+C_{22}-2C_{12}}.$$

From the elastic constants, we obtain the shear anisotropy factors for the tetragonal structure[70]

$$A_1 = A_2 = A_{\{100\}} = \frac{4C_{44}}{C_{11}+C_{33}-2C_{13}},$$
$$A_3 = A_{\{001\}} = \frac{2C_{66}}{C_{11}-C_{12}}.$$

The calculated anisotropy factors are tabulated in Table 4. The small anisotropy may minimize cracking propagation during sample preparation.[71] The elastic anisotropy is closely related to the inter-atomic bond strength.

Klemman[72] introduced an important parameter called internal strain parameter ξ, which describes the relative positions of the cation and anion sub-lattices under volume conserving strain distortions, for which positions are not fixed by symmetry[73] using the relation tendency of bond bending to bond stretching. It is defined as

$$\xi = \frac{C_{11}+8C_{12}}{7C_{11}+2C_{12}},$$

and its value usually lies between 0, showing minimum bond bending, and 1, showing minimum bond stretching.[74] Our calculated ξ are tabulated in Table 4. It shows that bond bending is preferred in these materials and this tendency is greater in m-$BiVO_4$ than the others.

Finally, we analyze the hardness of these materials by adopting the empirical scheme[75] which correlates Vicker's hardness H_v and Pugh's ratio k via the formula

$$H_v = 2(k^2G)^{0.585} - 3, \quad k = G/B.$$

The calculated values are tabulated in Table 4. It is seen that m-$BiVO_4$ is harder than the others. It is also observed that all the elastic properties are strongly agreed with the electronic properties.

3.4. Thermodynamical stability

In this paper, we used the thermodynamic property to describe the structural stabilities of different polymorphs of $BiVO_4$ with the elevated temperature.

Gibbs free energy G is one of the most important thermodynamic parameters to describe the stability of a compound. The variations of Gibbs free energy of different polymorphs of $BiVO_4$ with temperature are shown in Fig. 4. From the figure, it is found that the Gibbs free energy at the same temperature gradually decreases in the sequence: op > zt > m > st-$BiVO_4$. The smaller Gibbs free energy is favorable for the thermodynamic stability of the compound.[76] From this point of view, the thermal stabilities of these compounds gradually increase in the sequence: op > zt > m > st-$BiVO_4$. The rapid change of Gibbs free energy with temperature is logical for semiconductor crystal.[77]

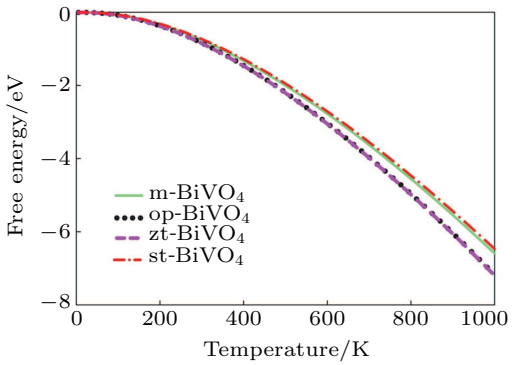


Fig. 4. (color online) Temperature dependent free energy of different $BiVO_4$ polymorphs.

Debye temperature θ_D is another thermodynamic parameter, at which all the phonon vibrations have the same frequency. It is also used to distinguish between high and low temperature regions for a solid. The Debye temperature is a suitable parameter to describe phenomena of solid-state physics which are associated with lattice vibration, elastic constants, specific heat, and melting point. The temperature dependent Debye temperatures for $BiVO_4$ polymorphs are shown in Fig. 5. The observed Debye temperatures of m-$BiVO_4$, op-$BiVO_4$, zt-$BiVO_4$, and st-$BiVO_4$ are 243.12 K, 146.83 K, 125.83 K, and 166.49 K, respectively at 0 K. At low temperature, the vibrational excitations arise solely from acoustic vibrations and the Debye temperature can also be calculated from elastic constants using the following equations:[78]

$$\theta_D = \frac{h}{k_B}\left[\frac{3n}{4\pi}\left(\frac{N_A\rho}{M}\right)\right]^{1/3} v_m,$$

where,

$$v_m = \left[\frac{1}{3}\left(\frac{2}{v_t^2}+\frac{1}{v_l^2}\right)\right]^{-1/3},$$

$$v_t = \sqrt{\frac{G}{\rho}}, \quad v_l = \sqrt{\left(B+\frac{4}{3}G\right)\frac{1}{\rho}}.$$

The calculated v_l, v_t, v_m, and θ_D using the elastic constants for different polymorphs of $BiVO_4$ are tabulated in Table 5 and the sequence of θ_D is st > m > op > zt-$BiVO_4$, which is consistent with the observed trend of Young's and shear moduli and also with thermodynamic data.

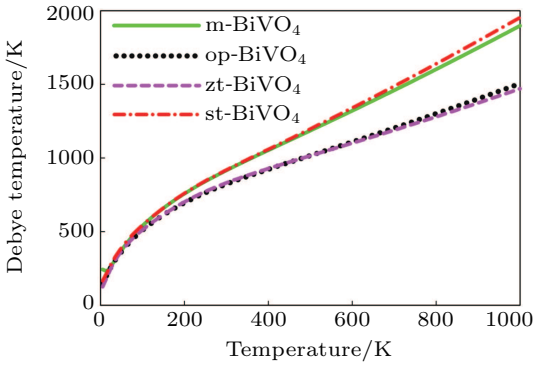


Fig. 5. (color online) Temperature dependent Debye temperature of different $BiVO_4$ polymorphs.

Table 5. Calculated volume V (Å^3), density ρ (kg·m^{-3}), longitudinal v_l (m·s^{-1}), transverse v_t (m·s^{-1}), and average sound velocity v_m (m·s^{-1}), Debye temperature θ_D (K), and Gruneisen parameter γ of different $BiVO_4$ polymorphs.

Polymorphs	V	ρ	v_l	v_t	v_m	θ_D	γ
m-$BiVO_4$	298	7.22	4986	2687	2999.65	242.94	1.744
op-$BiVO_4$	323	6.64	5029	2711	3026.46	238.57	1.743
zt-$BiVO_4$	349	6.17	5170	2607	2923.46	224.71	1.971
st-$BiVO_4$	309	6.97	5453	2843	3180.82	254.58	1.859

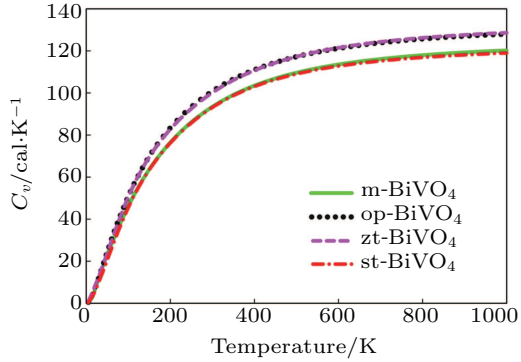


Fig. 6. (color online) Temperature dependent constant-volume heat capacity C_v of different $BiVO_4$ polymorphs.

Debye temperature θ_D is known as an important parameter closely related to many physical properties such as specific heat and melting temperature. The specific heat capacity C_v at constant volume for $BiVO_4$ polymorphs as a function of temperature is calculated and shown in Fig. 6. It is seen that C_v increases with increasing temperature. These results indicate that phonon thermal softening occurs when the temperature is raised. At the low temperature limit, C_v of all $BiVO_4$ polymorphs obeys the expected Debye T^3 law. At high temperature ($T \sim 840$ K), it follows the Dulong and Petit law and C_v approaches the classical asymptotic limit. These natures

of the curves indicate that atomic interactions in $BiVO_4$ polymorphs especially occur at low temperature. The heat capacity of a substance not only provides essential insight into its vibrational properties, but is also mandatory for many applications.

The Gruneisen parameter γ is often referred to as a temperature dependent anharmonicity parameter that reflects how many phonon vibrations in a crystal lattice deviate from harmonic oscillation. It also describes how the thermal properties of the material vary with the unit cell size. Anharmonicity of the chemical bond drives the phonon–phonon umklapp and normal processes that limit the lattice thermal conductivity.[79] The Gruneisen parameter γ of $BiVO_4$ polymorphs has been calculated using the following relation:[80]

$$\gamma = \frac{3}{2}\left(\frac{1+\nu}{2-3}\right),$$

where the Poisson ratio ν can be derived from the longitudinal (v_l) and transverse (v_t) sound waves using the following relation:[80,81]

$$\nu = \frac{1-2\left(v_t/v_l\right)^2}{2-2\left(v_t/v_l\right)^2}.$$

The calculated Gruneisen parameters of $BiVO_4$ are tabulated in Table 5 and their values increase in the order of zt > st > m > op-$BiVO_4$. The high γ results in low thermal conductivity and indicates a degree of anharmonicity in a crystal lattice of $BiVO_4$ which may be associated with the presence of trivalent Bi.[82]

4. Conclusion

To study the structural, mechanical stability, electronic and thermodynamic properties of $BiVO_4$ polymorphs, we employed first principles calculations with GGA. Our calculated optimized lattice parameters of this compound are in good agreement with the available theoretical and experimental results. From the band structure, it is revealed that m-$BiVO_4$, op-$BiVO_4$, and st-$BiVO_4$ structures are indirect band gap materials, while zt-$BiVO_4$ is a direct band gap material. Mulliken charge analysis indicates that all the polymorphs are mixed covalent-ionic in nature. The presence of a lone pair in m-$BiVO_4$ makes it a good candidate for photocatalytic application. The obtained elastic properties indicate that all polymorphs are mechanically stable and st-$BiVO_4$ possesses more ductile (ionic) properties. These technologically promising compounds are hard materials due to their higher bulk , Young's, and shear moduli. The lower shear anisotropic factors indicate smaller elastic anisotropy. The Gibbs free energy, Debye temperature, heat capacity, and Grüneisen parameter have been derived from the calculated elastic constants, which are essential for thin film growth of $BiVO_4$. The calculated thermodynamic properties confirm their thermodynamical stability and are also consistent with the elastic properties. The results recommend that $BiVO_4$ has potential structural and photocatalytic applications in various forms such as a nano-material. From our investigation, we conclude that m-$BiVO_4$ is useful for photocatalysts, solid state electrolyte, and electrode, on the other hand other polymorphs of $BiVO_4$ are applicable in electronic device fabrications. Our study would be helpful to the scientific community to select their application areas according to their desired properties.

References

[1] Hoffman M R, Martin S T, Choi W and Bahnemann D W 1995 *Chem. Rev.* **95** 69
[2] Chen X and Mao S S 2007 *Chem. Rev.* **107** 2891
[3] Kudo A, Omori K and Kato H 1999 *J. Am. Chem. Soc.* **121** 11459
[4] Yu J and Kudo A 2006 *Adv. Funct. Mater.* **16** 2163
[5] Tokunaga S, Kato H and Kudao A 200 *Chem. Mater.* **13** 4624
[6] Zhang L W, Wang Y J, Cheng H Y, Yao W Q and Zhu Y 2009 *Adv. Mater.* **21** 1286
[7] Amano F, Yamakata A, Nogmi K, Osawa M and B Ohtani 2008 *J. Am. Chem. Soc.* **130** 17650
[8] Long M, Cai W and Kisch H 2008 *Chem. Phys. Lett.* **461** 102
[9] Ke D N, Peng J Y, Ma L, Cai P and Dai L 2009 *Inorg. Chem.* **48** 4685
[10] Abraham F, Debreuille-Gresse M F, Mairesse G and Nowogrocki G 1988 *Solid State Ionics* **28–30** 529
[11] Baker T L, Faber K T and Readey D W 1991 *J. Am. Chem. Soc.* **74** 1619
[12] Sleight A W, Chen H Y, Ferretti A and Cox D E 1979 *Meter. Res. Bull.* **14** 1571
[13] Walsh A, Yan Y, Huda M N, Al-Jassim M M and Wei S H 2009 *Chem. Mater.* **21** 547
[14] Liu Y, Huang B, Dai Y, Zhang X, Qin X, Jiang M and Whangbo M H 2009 *Catal. Commun.* **11** 210
[15] Li G, Zhang D and Yu J 2008 *Chem. Mater.* **20** 3983
[16] Sayama K, Nomura A, Zou Z, Abe R, Abe Y and Arakawa H 2003 *Chem. Commun.* **16** 2908
[17] Sayama K, Nomura A, Arai T, Sugita T, Abe R, Yanagida M, Oi T, Iwasaki Y, Abe Y and Sugihara H 2006 *J. Phys. Chem. B* **110** 11352
[18] Dunkle S S, Helmich R J and Suslick K S 2009 *J. Phys. Chem. C* **113** 11980
[19] Luo H, Mueller A H, McCleskey T M, Burrell A K, Bauer E and Jia Q X 2008 *J. Phys. Chem. C* **112** 6099
[20] Yu J Q, Zhang Y and Kudo A 2009 *J. Solid. State. Chem.* **182** 223
[21] Xie Y, Zhu Y, Yan S and Wang S X 2006 *Chemistry-A Eueropean Journal* **14** 1601
[22] Neves M C and Trindade T 2002 *Thin Solid Films* **406** 93
[23] Zhou L, Wang W Z, Liu S W, Zhang L S, Xu H L and Zhu W 2006 *J Mol Cata. A: Chemical* **252** 120
[24] Sun Y, Wu C, Long R, Cui Y, Zhang S and Xie Y 2009 *Chem. Cummun.* **30** 4542
[25] Sun Y, Xie Y, Wu C and Long R 2010 *Cryst. Growth Des.* **10** 602
[26] Shang M, Wang W, Sun S, Ren J, Zhou L and Zhang L 2009 *J. Phys. Chem. C* **113** 20228
[27] Su J, Guo L, Yoriya S and Grimes C A 2010 *Cryst. Growth. Des.* **10** 856
[28] Yu J and Kudo A 2005 *Chem. Lett.* **34** 850
[29] Zhang L, Chen D and Jiao X 2006 *J. Phys. Chem. B* **110** 2668
[30] Xi G and Ye J 2010 *Chem. Commun.* **46** 1893
[31] Zhao Y, Xie Y, Zhu X, Yan Sand Wang S 2008 *Chem. Eur. J.* **14** 1601
[32] Zhou L, Wang W and Xu H 2008 *Cryst. Growth. Des.* **8** 728
[33] Luo H, Mueller A H, McClesky T M, Burrell A K, Bauer E and Jia Q X 2008 *J. Phys. Chem. C* **112** 6099
[34] Castillo N C, Ding L, Graule T and Pulgarin C 2010 *J. Photochem. Photobiol. A: Chem.* **216** 221
[35] Yin H, Sun Y, Shi D, Wang X and Wang L 2011 *Int. J. Phys. Sci.* **6** 4287
[36] Garcia Perez U M, Sepulveda-Guzman S, Martinez-de la Cruz A and Ortiz Mendez U 2011 *J Mol Catal A: Chem* **335** 169
[37] Yin W J, Wei S H, Al-Jassim M M, Turner J and Yan Y 2011 *Phys. Rev. B* **83** 155102
[38] Zhou B, Qu J, Zhao X and Liu H 2011 *J. Environ. Sci.* **23** 151
[39] Kudo A, Ueda K, Kato and Mikami H 1998 *Catal. Lett.* **53** 229

[40] Kothani S, Koshiko M, Kudo A, Tokumura K, Ishigaki Y, Toriba A, Hayakawa K and Nakagaki R 2003 *Appl. Catal. B* **46** 573

[41] Kothani S, Hiro J, Yamamoto N, Kudo A, Tokumura K and Nakagaki R 2005 *Catal. Commun.* **6** 185

[42] Zhang X, Ai Z, Jia F, Zhang L, Fan X and Zou Z 2007 *Mater. Chem. Phys.* **103** 162

[43] Perdew J P, Ruzsinszky A, Csonka G I, Vydrov O A, Scuseria G E, Constantin L A, Zhou X and Burke K 2008 *Phys. Rev. Lett.* **100** 136406

[44] Heyd J, Scuseria G E and Ernzerhof M 2003 *J. Chem. Phys.* **118** 8207

[45] Paier J, Marsman M and Hummer K 2006 *J. Chem. Phys.* **125** 249901

[46] Heyd J, Scuseria G E and Ernzerhof M 2006 *J. Chem. Phys.* **124** 219906

[47] Yuan Y, Huang Y, Ma F, Zhang Z, Wei X and Zhu G 2016 *J. Mater. Sci.* **51** 6662

[48] Segall M D, Lindan P, Probet M J, Pickard C J, Hasnip P J, Clark S J and Payne M C 2002 *J. Phys.: Condens. Matter* **14** 2717

[49] Fagan S B, Mota R and Baierle R J 2001 *J. Mol. Struct.* **539** 101

[50] Perdew J P, Burke K and Ernzerhof M 1996 *Phys. Rev. Lett.* **77** 3865

[51] Qurashi M M and Bernes W H 1952 *Am. Mineralogist* **37** 423

[52] Kweon K E and Hwang G S 2012 *Phys. Rev. B* **86** 165209

[53] Ding K, Chen B, Fang Z and Zhang Y 2013 *Theor. Chem. Acc.* **132** 1352

[54] Dreyer G and Tillmanns E 1981 *Neues. Jb. Miner.* 151

[55] Kweon K E and Hwang G S 2013 *Appl. Phys. Lett.* **103** 131603

[56] Wu Z J, Zhao E J, Xiang H P, Hao X F and Liu X J 2007 *J. Meng. Phys. Rev. B* **76** 054115

[57] Jun L Q, Chao Z N, Sheng L F and Tang L Z 2014 *Chin. Phys. B* **23** 047101

[58] Beckstein O, Klepeis J E, Hart G L W and Pankratow O 2001 *Phys. Rev. B* **63** 134112

[59] Wallace D C 1972 *Thermodynamics of Crystals* (New York: Wiley)

[60] Piskunov S, Heifets E, Eglitis R I and Borstel G 2004 *Comput. Mater. Sci.* **29** 165

[61] Voigt W 1928 *Lehrbuch der Kristallphysik Leipzig: Teubner* 574

[62] Reuss A and Angew Z 1929 *Math. Mech.* **9** 49

[63] Hill R 1952 *Proc. Phys. Soc. A* **65** 349

[64] Hill R 1963 *J.Mech. Phys. Solids* **11** 357

[65] Kumar V, Shrivastava A K and Jha V 2010 *J. Phys. Chem. Solids* **71** 1513

[66] Pugh S F 1954 *Philos. Mag.* **45** 823

[67] Jenkins C H and Khanna S K 2005 *Mech. Materials* **5** 62

[68] Bilal M, Shafiq M, Ahmad I and Khan I 2014 *J. Semicond.* **35** 072001

[69] Han Y Y, Mei G Z, Duo H H and Qun W 2013 *Solids States Sciences* **18** 17

[70] Yildirim A, Koc H and Deligoz E 2012 *Chin. Phys. B* **21** 037101

[71] Yi W, Qing X and Yan Y 2010 *J. Cent South Univ.* **21** 500

[72] Kleinman L 1962 *Phys. Rev.* **128** 2614

[73] Harrison W A 1989 *Electronic Structure and Properties of Solid*s (New York: Dovor)

[74] Sverdlov V 2011 *Strain Induced Effects in Advanced MOSFETs* (New York: Springer)

[75] Chen X Q, Niu H, Li D and Li Y 2011 *Intermetallic* **19** 1275

[76] Shi D M, Wen B and Melnik R 2009 *J. Solid State Chem.* **128** 2664

[77] Georgobiani A N and Sheykman M K 1986 *Physics Compounds* (Moscow: AIIBVI Nauka)

[78] Deligoz E, Ciftci Y O and Jochym P T 2008 *Mater. Chem. Phys.* **111** 29

[79] Loffe A F 1958 *Physics of Semiconductors Infosearch*

[80] Sanditov D S and Belomestnykh V N 2011 *Tech. Phys.* **56** 1619

[81] Wan C L, Pan W, Xu Q, Qin Y X, Wang J D, Qu Z X and Fang M H 2006 *Phys. Rev. B* **74** 144109

[82] Skoug E J, Cain J D and Morelli D T 2010 *Appl. Phys. Lett.* **96** 181905